

## Lead-tellurium oxysalts from Otto Mountain near Baker, California: I. Ottoite, $\text{Pb}_2\text{TeO}_5$ , a new mineral with chains of tellurate octahedra

ANTHONY R. KAMPF,<sup>1,\*</sup> ROBERT M. HOUSLEY,<sup>2</sup> STUART J. MILLS,<sup>3</sup> JOSEPH MARTY,<sup>4</sup>  
AND BRENT THORNE<sup>5</sup>

<sup>1</sup>Mineral Sciences Department, Natural History Museum of Los Angeles County, 900 Exposition Blvd., Los Angeles, California 90007, U.S.A.

<sup>2</sup>Division of Geological and Planetary Sciences, California Institute of Technology, Pasadena, California 91125, U.S.A.

<sup>3</sup>Department of Earth and Ocean Sciences, University of British Columbia, Vancouver, British Columbia V6T 1Z4, Canada  
<sup>4</sup>3457 E. Silver Oak Road, Salt Lake City, Utah 84108, U.S.A.

<sup>5</sup>3898 S. Newport Circle, Bountiful, Utah 84010, U.S.A.

### ABSTRACT

Ottoite,  $\text{Pb}_2\text{TeO}_5$ , is a new tellurate from Otto Mountain near Baker, California. Most of the mining on Otto Mountain occurred between 1940 and 1970 and is attributed to Otto Fuetterer, for whom the mountain is now named. The new mineral occurs on fracture surfaces and in small vugs in brecciated quartz veins, which intersect granitic rocks. Ottoite is directly associated with acanthite, bromine-rich chlorargyrite, gold, iodargyrite, khinite, wulfenite, and four other new tellurates: housleyite, mark-cooperite, thorneite, and timroseite. Various other secondary minerals occur in the veins, including two other new secondary tellurium minerals, paratimroseite and telluroperite. Ottoite and most other secondary minerals of the quartz veins are interpreted as having formed from the partial oxidation of primary sulfides and tellurides during or following brecciation of the veins. A later generation of quartz mineralization then recemented the breccias, effectively isolating and protecting the secondary mineralization from further alteration. Ottoite is monoclinic, space group  $I2/a$ , with the unit cell:  $a = 7.5353(6)$ ,  $b = 5.7142(5)$ ,  $c = 10.8981(12)$  Å,  $\beta = 91.330(6)^\circ$ ,  $V = 469.13(8)$  Å<sup>3</sup>, and  $Z = 4$ . The mineral occurs as complex spear-shaped crystals in subparallel to divergent intergrowths. It is yellow and transparent to translucent, with a pale yellow streak and adamantine luster. Mohs hardness is estimated at 3. The mineral is brittle, with an irregular fracture and two cleavages in the [100] zone at  $\sim 90^\circ$ —possibly on {010} and {001}. The calculated density is 8.721 g/cm<sup>3</sup>. Ottoite is biaxial (–), with a large  $2V$ , but indices of refraction are too high to be measured. The optic orientation could only partially be determined:  $Y \approx a$ . No pleochroism was observed. Electron microprobe analyses provided the following averages: PbO 68.88 and TeO<sub>3</sub> 28.03, total 96.95 wt%; the empirical formula (based on O = 5) is  $\text{Pb}_{1.96}\text{Te}_{1.01}^{6+}\text{O}_5$ . The strongest powder X-ray diffraction lines are [ $d_{\text{obs}}$  in Å ( $hkl$ )  $I$ ]: 3.131 ( $\bar{2}02$ ) 64, 3.055 (013) 90, 3.015 (211) 100, 2.112 ( $\bar{2}22$ ) 29, 1.810 (006,  $\bar{2}15$ ) 21, 1.773 ( $\bar{4}11$ , 402) 43, 1.686 (033, 231) 20. The crystal structure ( $R_1 = 0.020$ ) consists of straight chains of *trans*-corner-sharing  $\text{Te}^{6+}\text{O}_6$  octahedra parallel to  $a$ , which are joined by bonds to Pb atoms. The Pb atom exhibit markedly lopsided 11-coordination, typical of  $\text{Pb}^{2+}$  with stereoactive  $6s^2$  lone-pair electrons. The powder X-ray diffraction pattern of ottoite is very similar to that reported for girdite. Examination of girdite type material suggests that its description was based upon data obtained from at least two and possibly three different phases, one of which may correspond to ottoite.

**Keywords:** Ottoite, girdite, new mineral, tellurate, crystal structure, stereoactive lone-pair, Otto Mountain, California

### INTRODUCTION

The Mojave Desert in the U.S. Southwest contains literally thousands of old mines and prospects, the vast majority of which were never economically profitable. However, a few deposits, though they produced little ore, have yielded a noteworthy variety of rare and unusual minerals. One such deposit, the Blue Bell claims in the Soda Mountains, about 11 km west of Baker, San Bernardino County, California, has been a prolific producer of micro-crystals of rare species for six decades (Crowley 1977; Maynard et al. 1984; Kampf et al. 2009; Mills et al. 2010).

\* E-mail: akampf@nhm.org

The fairly recent discovery of the tellurate minerals kuksite and quetzalcoatlite (originally misidentified as thalocite) at the Blue Bell claims (Housley 1997) naturally led to the investigation of other nearby mining sites in the Soda Mountains in the hopes of finding additional tellurate locations. In early 2004, small bright green crystals of khinite were found at the Aga mine on Otto Mountain (Fig. 1). Within six months, several other secondary tellurium phases turned up there that appeared to be new species on the basis of semi-quantitative SEM-EDS analysis. The extreme rarity and small crystal size of these secondary tellurium minerals has made the recovery of adequate material for characterization slow, painstaking work. Continuing efforts

have now yielded a total of seven new species, and additional possibly new phases remain under study.

This paper, the first in a series on the secondary tellurium minerals of Otto Mountain, describes the new mineral species ottoite, provides background information on the geology and mining history of the area, and discusses the paragenesis and mineral associations. Ottoite is named for the locality, Otto Mountain. The new mineral and name have been approved by the Commission on New Minerals, Nomenclature and Classification of the International Mineralogical Association (IMA 2009-063). Five cotype specimens are deposited in the Natural History Museum of Los Angeles County, catalog numbers 62511, 62512, 62528, 62529, and 62530.

## GEOLOGY AND MINING HISTORY

What is now shown as Otto Mountain on USGS maps (Fig. 2) is actually a hill about 2.5 km across, about 2.5 km northwest of Baker, California. It is considered part of the Soda Mountains. The geology in this part of the Soda Mountains has been mapped in considerable detail by Grose (1959). Otto Mountain consists largely of granitic rocks (granodiorite and quartz diorite), but has small roof pendants of carbonates on the southeast ridge and a gneiss complex on the northeast side extending over the top of the mountain. Stratigraphically above the gneiss near the northeast base, more carbonate is exposed. Grose (1959) considered the gneiss to be Precambrian and the carbonate to also be "old." He



FIGURE 1. Otto Mountain viewed from the southeast. The adit at the base of the mountain at the center is the Aga mine.

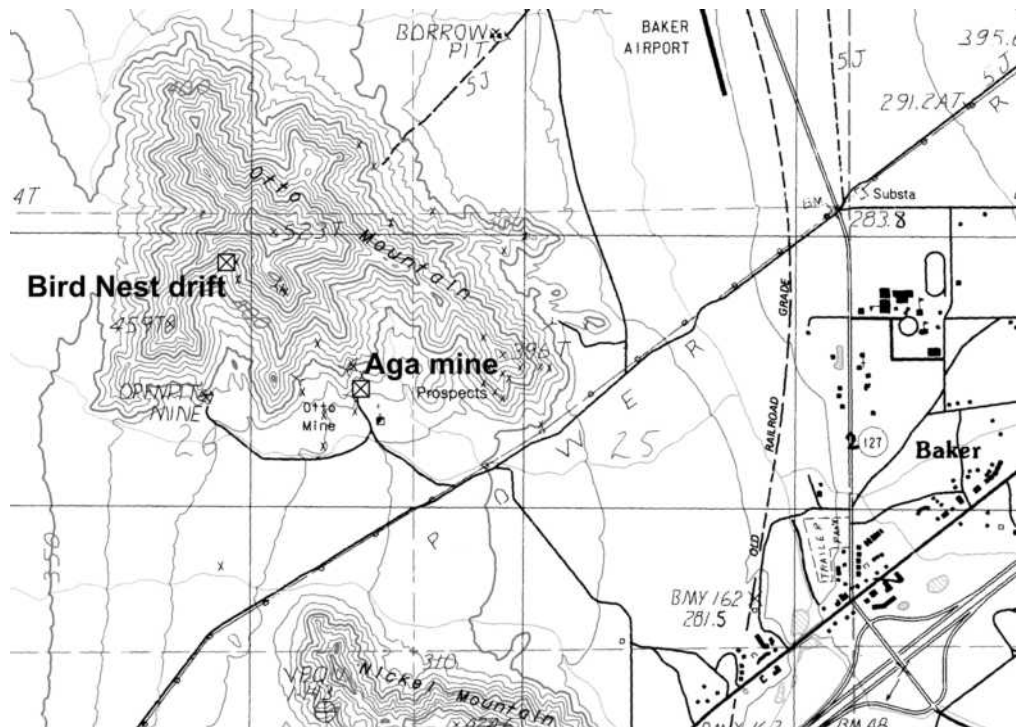


FIGURE 2. Portion of the 7.5 min USGS topographic map of the Baker quadrangle showing the locations of the Aga mine (aka. Otto mine) and Bird Nest drift.

also considered the granitic rocks to be pre-Tertiary in age and later workers (e.g., Walker and Wardlaw 1989) suggest they date to ~100 Ma.

The granitic rocks on the southwest side of the mountain are cut by a small group of sub-parallel quartz veins that generally trend northwest-southeast. Individual quartz veins are rarely over half a meter in thickness, but some can be traced for over 200 m, and they are conspicuous in outcrop in many places.

The most recent mining history of the area appears to have started in 1940 when Otto Fuetterer, for whom the mountain is now named, filed six claims named Good Hope 1–6. A short time later, A.G. Andrews (AGA) filed adjacent claims named Aga 1–20. Sometime after 1950, Fuetterer became sole owner of all of the claims, continuing to work them and ship small amounts of ore until his death around 1970.

Today, about two dozen workings of various sizes can be found on Otto Mountain, with adits ranging in length from about a meter to 300 m. The quartz veins have scattered areas containing up to a few percent sulfides or calcite as small blebs, usually <5 cm across, disseminated in the quartz, but no sulfide ore body was ever encountered. The most prominent working is an adit on the south side of Otto Mountain labeled “Aga Mine” on the USGS 15 min Baker quadrangle map and “Otto Mine” on the 7.5 min map. It was here that khinite and other secondary tellurium minerals were first noted by one of the authors (R.M.H.) in January of 2004. In June 2004, one of the other authors (J.M.) found secondary tellurium minerals in a short drift about 0.7 km northwest of the aforementioned site. This site was dubbed the Bird Nest drift by J.M.

The name ottoite, given for the locality name, also indirectly honors Otto Fuetterer, and rightfully so, for without his considerable efforts in exposing the unusual mineralization in the quartz veins on the mountain, ottoite and at least six other new secondary tellurium minerals would not have been discovered.

## OCCURRENCE

Ottoite was found at the Aga mine (35° 16.399'N 116° 05.665'W) on Otto Mountain, ~2 km northwest of Baker, San Bernardino County, California, U.S.A., and in the Bird Nest drift on the southwest flank of Otto Mountain 0.7 km northwest of the Aga mine (35° 16.606'N 116° 05.956'W).

Ottoite is rare and occurs on fracture surfaces and in small vugs in quartz veins. Species observed in direct association with the new mineral include acanthite, bromine-rich chlorargyrite, gold, iodargyrite, khinite, wulfenite, and four other new minerals: housleyite [Pb<sub>6</sub>CuTe<sub>4</sub>O<sub>18</sub>(OH)<sub>2</sub>] (IMA2009-024; Kampf et al. 2010b), markcooperite [Pb<sub>2</sub>(UO<sub>2</sub>)TeO<sub>6</sub>] (IMA2009-045; Kampf et al. 2010c), thorneite [Pb<sub>6</sub>(Te<sub>2</sub>O<sub>10</sub>)(CO<sub>3</sub>)Cl<sub>2</sub>(H<sub>2</sub>O)] [IMA2009-023; Kampf et al. (2010a)], and timroseite [Pb<sub>2</sub>Cu<sub>5</sub><sup>2+</sup>(Te<sup>6+</sup>O<sub>6</sub>)<sub>2</sub>(OH)<sub>2</sub>] [IMA2009-064; Kampf et al. (2010d)]. Other species identified in the assemblages include: anglesite, atacamite, boleite, brochantite, burckhardtite, calcite, caledonite, celestine, cerussite, chalcopyrite, chrysocolla, devilline, diaboleite, fluorite, formacite, galena, goethite, hessite, jarosite, kuranakhite, linarite, malachite, mimetite, mottramite, munakataite, murdochite, muscovite, perite, phosphohedyphane, plumbojarosite, pyrite, schiefelinite, vanadinite, vauquelinite and two other new minerals: paratimroseite [Pb<sub>2</sub>Cu<sub>4</sub><sup>2+</sup>(Te<sup>6+</sup>O<sub>6</sub>)<sub>2</sub>(H<sub>2</sub>O)<sub>2</sub>] [IMA2009-065; Kampf et al. (2010d)] and telluroperite [Pb<sub>3</sub>Te<sup>4+</sup>O<sub>4</sub>Cl<sub>2</sub>] [IMA2009-044;

Kampf et al. (2010e)]. Other potentially new species are still under investigation.

In addition to the secondary tellurium minerals, quite a large number of mineral species occur in the quartz veins of Otto Mountain. It thus becomes even more interesting to try to understand the paragenesis. Several field observations seem relevant:

(1) Individual sulfide blebs in the quartz are generally well separated and rarely exceed 2 cm in diameter, and the same can be said for primary calcite crystals. The sulfide blebs can consist of pure galena, pyrite, or chalcopyrite, or combinations of two or more of these. Hessite (Ag<sub>2</sub>Te) can occur with the sulfides or as sub-millimeter isolated grains in the quartz. Sub-millimeter grains of free gold are occasionally seen. Sphalerite has only been found in one small section of the quartz veins and one single grain of tetradymite has been observed.

(2) The quartz veins themselves have been highly brecciated and in many cases contain open space between the fragments. A later generation of quartz recements the breccias and in many cases heals fracture surfaces with a new layer of quartz.

(3) Khinite frequently occurs within millimeters of unoxidized galena.

(4) Khinite also frequently occurs embedded in the late-stage clear quartz.

(5) Primary sulfides and khinite can both be found in rocks exposed in surface outcrops.

From the above observations we infer that the secondary tellurium minerals, as well as the other secondary minerals, formed in a multitude of local micro-environments that resulted from the partial oxidation of the primary sulfides during or following brecciation of the veins. The Te would have been provided by the oxidation of hessite and perhaps other, as yet unrecognized, tellurides. The later generation of quartz mineralization then recemented the breccias, effectively isolating and protecting from further alteration the delicate secondary minerals, as well as the remaining sulfides.

## PHYSICAL AND OPTICAL PROPERTIES

The mineral occurs as complex spear-shaped crystals, elongate on *a*, in subparallel to divergent intergrowths up to about 0.5 mm long (Fig. 3). The complex shape of the crystals, consisting of numerous indistinct and often rounded forms, and the necessity to split the crystals into small fragments for single-crystal work made it impossible to conduct a morphological study using an optical goniometer. Using the SHAPE crystal drawing program (Dowty 2008) to simulate the morphologies of the more distinct crystals in SEM images (Fig. 4), allowed the determination of the likely crystal forms: {110}, {111}, {102}, {102}, {011}, {011}, and {111} (Fig. 5). Merohedral twinning is indicated by structure analysis (see below).

Ottoite is yellow and transparent to translucent, with a pale yellow streak and adamantine luster. It is nonfluorescent. The Mohs hardness is estimated at 3. The mineral is brittle, with an irregular fracture and two cleavages in the [100] zone at ~90°—possibly on {010} and {001}. The density could not be measured because it is greater than those of available high-density liquids and there is insufficient material for physical measurement. The density calculated for the empirical formula is 8.721 g/cm<sup>3</sup> and for the ideal formula 8.805 g/cm<sup>3</sup>.

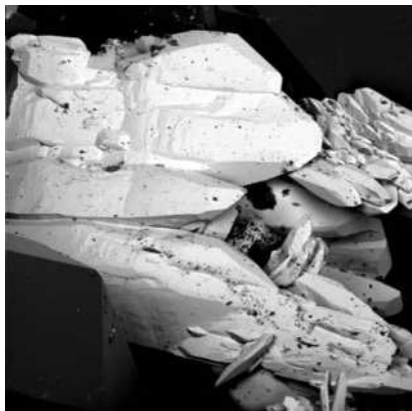


FIGURE 3. Backscatter SEM image of ottoite crystals (FOV 350  $\mu\text{m}$ ).



FIGURE 4. Backscatter SEM image of ottoite crystals (FOV 50  $\mu\text{m}$ ).

The indices of refraction exceed those of available index fluids. The Gladstone-Dale relationship (Mandarino 1981) predicts  $n_{\text{av}} = 2.258$  based on the empirical formula. Orthoscopic and conoscopic optical examination using a Leitz Ortholux I polarizing microscope equipped with a Supper spindle stage showed ottoite to be biaxial (–), with a large  $2V$ . The poor quality of the conoscopic figure did not permit accurate determination of  $2V$  or observation of the dispersion. The optic orientation could only partially be determined:  $Y \approx a$ . No pleochroism was observed.

In dilute HCl, ottoite immediately decomposes, turning opaque white, expanding, and leaving an insoluble crystalline residue of  $\text{PbCl}_2$  (cotunnite).

### CHEMISTRY

Five chemical analyses carried out using a JEOL8200 electron microprobe (WDS mode, 15 kV, 10 nA, 20  $\mu\text{m}$  beam diameter) at the Division of Geological and Planetary Sciences, California Institute of Technology, provided the averages (and ranges): PbO 68.88 (68.27–69.74) and  $\text{TeO}_3$  28.03 (27.78–28.19), total 96.95 (96.05–97.88) wt%. No other elements were detected in EDS analyses. Elements Cl, S, Cr, Cu, Bi, and U were below the microprobe detection limits. Note that the crystals are prone to electron beam damage. This and sample porosity contributes to the low analytical total, even though we used the mildest analytical conditions feasible. This problem of sample instability in the electron beam appears to be common in tellurates (cf. Grundler et al.

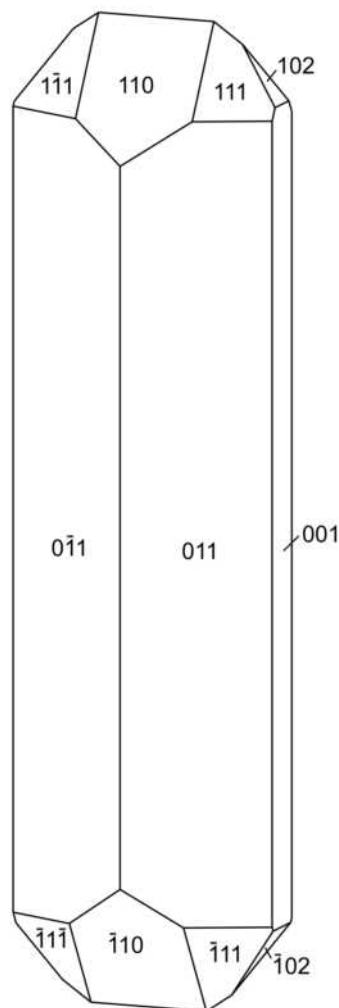


FIGURE 5. Crystal drawing of ottoite in non-standard orientation with a vertical (clinographic projection).

2008; Mills et al. 2008, 2009b, 2010). The structure determination and bond valence considerations (see below) indicate the absence of OH,  $\text{H}_2\text{O}$ , and  $\text{CO}_2$  in ottoite.

The empirical formula (based on O = 5) is  $\text{Pb}_{1.96}\text{Te}_{1.01}^{6+}\text{O}_5$ . The simplified formula (based on O = 5) is  $\text{Pb}_2\text{TeO}_5$ , which requires PbO 71.77 and  $\text{TeO}_3$  28.23, total 100.00 wt%.

### X-RAY CRYSTALLOGRAPHY AND STRUCTURE DETERMINATION

Both powder and single-crystal X-ray diffraction data were obtained on a Rigaku R-Axis Spider curved imaging plate microdiffractometer utilizing monochromatized  $\text{MoK}\alpha$  radiation. The powder data presented in Table 1 show good agreement with the pattern calculated from the structure determination.

The selection of a crystal fragment suitable for structure determination was challenging because all crystals occur in complex subparallel to divergent intergrowths and/or twins. Composite crystals were carefully split into smaller fragments and screened under crossed-polarizers and by collecting orientation frames on the diffractometer. The first crystal fragment on

which structure data were collected measured  $80 \times 45 \times 40 \mu\text{m}$ . Examination of the frames revealed no obvious evidence of twinning; however, weak satellite peaks were observed, indicating the presence of a small, slightly misaligned second crystal. The initial cell obtained,  $a = 13.099(3)$ ,  $b = 5.714(1)$ ,  $c = 7.520(2)$  Å,  $\beta = 123.80(3)^\circ$ , matched that of synthetic  $\text{Pb}_2\text{TeO}_5$ , whose structure was solved and refined in space group  $Cc$  from powder data using the Rietveld method by Wedel et al. (1998).

The Rigaku CrystalClear software package was used for processing of the structure data, including the application of an empirical absorption correction. The SHELXL-97 software (Sheldrick 2008) was used, with neutral atom scattering factors, for the refinement of the structure. Our initial attempt to refine the structure based upon the atomic coordinates and space group of Wedel et al. (1998) yielded  $R_1 = 0.034$  and  $wR_2 = 0.078$  for 751 reflections with  $F_o > 4\sigma F$ ; however, the anisotropic displacement parameters (ADPs) for two of the O atoms had non-positive definite values and the other O atoms exhibited very anisotropic shape.

Statistical analysis of the data using Platon (Speck 2001) and Rigaku XPlain space group tools suggested the transformed cell ( $a_{\text{new}} = c_{\text{old}}$ ,  $b_{\text{new}} = b_{\text{old}}$ ,  $c_{\text{new}} = -a_{\text{old}} - c_{\text{old}}$ ):  $a = 7.52$ ,  $b = 5.71$ ,  $c = 10.90$  Å, and  $\beta = 91.3^\circ$ , in the space group  $I2/a$ . After reintegration of the reflections and processing of the data, the structure was solved by direct methods using SIR92 (Altomare et al. 1994). The location of all atoms was straightforward and provided a structure virtually identical to our first attempt, but with improved  $R$  values ( $R_1 = 0.028$  and  $wR_2 = 0.076$  for 414 reflections with  $F_o > 4\sigma F$ ) and no anomalous ADPs; however, there were numerous systematic absence violations. After unsuccessful attempts to refine the structure in other space groups, our conclusion was that the space group violations were probably due to merohedral twinning.

**TABLE 1.** X-ray powder diffraction data for ottoite

$l_{\text{obs}}$	$d_{\text{obs}}$	$d_{\text{calc}}$	$l_{\text{calc}}$	$hkl$
4	5.060	5.068	6	011
64	3.131	3.133	53	202 *
90	3.055	{ 3.071 3.068	{ 4 100	{ 202 013 *
100	3.015	3.011	95	211 *
19	2.871	2.862	41	020 *
19	2.186	2.187	21	204 *
29	2.112	{ 2.113 2.094	{ 40 4	{ $\bar{2}22$ * 222
21	1.810	{ 1.817 1.808	{ 13 24	{ 006 $\bar{2}15$ *
43	1.773	{ 1.773 1.770	{ 26 11	{ 411 * 402
13	1.739	1.738	19	224 *
20	1.686	{ 1.689 1.680	{ 21 21	{ 033 * 231 *
7	1.568	1.567	7	404 *
8	1.533	1.534	15	026 *
12	1.504	1.506	12	422 *
3	1.429	1.431	5	040 *
6	1.385	1.386	9	217 *
18	1.372	{ 1.374 1.370	{ 11 10	{ 424 * 415 *
4	1.352	1.348	9	235 *
6	1.333	1.334	8	431 *
6	1.301	1.302	9	$\bar{2}42$ *

Notes:  $l_{\text{obs}}$  based upon peak heights.  $l_{\text{calc}}$  calculated from the crystal structure using Powder Cell (Kraus and Nolze 1996).  $d_{\text{calc}}$  based on the cell refined from the powder data (\*) using UnitCell (Holland and Redfern 1997). Refined cell:  $a = 7.5446(9)$ ,  $b = 5.7243(5)$ ,  $c = 10.9051(14)$  Å,  $\beta = 91.241(9)^\circ$ , and  $V = 470.85(6)$  Å<sup>3</sup>.

Further attempts to isolate an untwinned fragment, yielded a  $45 \times 35 \times 10 \mu\text{m}$  fragment that exhibited no obvious reflections violating the  $I2/a$  space group absences. Refinement of the structure from this data provided  $R_1 = 0.020$  and  $wR_2 = 0.048$  for 427 reflections with  $F_o > 4\sigma F$ . All ADPs were reasonable and only three relatively weak reflections were found to violate the space group absences. The details of the data collection and the final structure refinement are provided in Table 2. The final atomic coordinates and displacement parameters are in Table 3. Selected interatomic distances are listed in Table 4 and bond valences in Table 5. Note that structure factors and CIF data are on deposit<sup>1</sup>.

## DESCRIPTION OF THE STRUCTURE

The structure (Figs. 6 and 7) consists of straight chains of *trans*-corner-sharing  $\text{Te}^{6+}\text{O}_6$  octahedra parallel to  $c$ , which are joined by bonds to Pb atoms. The  $\text{Te}^{6+}\text{O}_6$  octahedron is relatively regular with O-Te-O angles ranging from  $87.6$  to  $92.4^\circ$ , but exhibits significant octahedral elongation in the direction of the chain, probably in response to repulsion between adjacent  $\text{Te}^{6+}$  cations. The Pb atom exhibits markedly lopsided coordination to 11 O atoms (Fig. 8), due the  $6s^2$  lone-electron-pair effect typically exhibited by  $\text{Pb}^{2+}$  (e.g., Moore 1988; Cooper and Hawthorne 1994; Kharisun et al. 1997; Mills et al. 2009a). In fact, the Pb atoms in the structures of all seven recently discovered new minerals from Otto Mountain exhibit this effect. The bond-valence analysis (Table 5) clearly indicates the absence of OH and  $\text{H}_2\text{O}$  in the structure.

<sup>1</sup> Deposit item AM-10-042, structure factors and CIF. Deposit items are available two ways: For a paper copy contact the Business Office of the Mineralogical Society of America (see inside front cover of recent issue) for price information. For an electronic copy visit the MSA web site at <http://www.minsocam.org>, go to the American Mineralogist Contents, find the table of contents for the specific volume/issue wanted, and then click on the deposit link there.

**TABLE 2.** Data collection and structure refinement details for ottoite

Diffractometer	Rigaku R-Axis Spider with curved imaging plate
X-ray radiation/power	$\text{MoK}\alpha$ ( $\lambda = 0.71075$ Å)/50 kV, 40 mA
Temperature	298(2) K
Formula	$\text{Pb}_2\text{TeO}_5$
Space group	$I2/a$
Unit-cell dimensions	$a = 7.5353(6)$ Å $b = 5.7142(5)$ Å $c = 10.8981(12)$ Å $\beta = 91.330(6)^\circ$
Z	4
Volume	$469.13(8)$ Å <sup>3</sup>
Density (for ideal formula)	$8.806$ g/cm <sup>3</sup>
Absorption coefficient	$77.696$ mm <sup>-1</sup>
$F(000)$	1024
Crystal size	$0.045$ mm $\times$ $0.035$ mm $\times$ $0.010$ mm
$\theta$ range	$4.03^\circ$ to $27.49^\circ$
Index ranges	$-8 \leq h \leq 9$ , $-7 \leq k \leq 7$ , $-14 \leq l \leq 14$
Reflections collected/unique	4774/535 [ $R_{\text{int}} = 0.0431$ ]
Reflections with $F_o > 4\sigma F$	427
Completeness to $\theta = 27.50^\circ$	99.4%
Max. and min. transmission	0.5105 and 0.1278
Refinement method	Full-matrix least-squares on $F^2$
Parameters refined	40
GoF	1.072
Final $R$ indices [ $F_o > 4\sigma F$ ]	$R_1 = 0.020$ , $wR_2 = 0.048$
$R$ indices (all data)	$R_1 = 0.027$ , $wR_2 = 0.051$
Largest diff. peak/hole	$0.945/-1.874$ e/Å <sup>3</sup>

Notes:  $R_{\text{int}} = \sum |F_o^2 - F_o^2(\text{mean})| / \sum F_o^2$ .  $\text{GoF} = S = \{ \sum [w(F_o^2 - F_c^2)] / (n - p) \}^{1/2}$ .  $R_1 = \sum |F_o - |F_c|| / \sum F_o$ .  $wR_2 = \{ \sum [w(F_o^2 - F_c^2)^2] / \sum [w(F_o^2)^2] \}^{1/2}$ .  $w = 1 / [\sigma^2(F_o) + (aP)^2 + bP]$  where  $a$  is 0.0160,  $b$  is 1.9903, and  $P$  is  $[2F_o^2 + \text{Max}(F_o, 0)]/3$ .

**TABLE 3.** Atomic coordinates and displacement parameters ( $\text{\AA}^2$ ) for ottoite

	x	y	z	$U_{eq}$	$U_{11}$	$U_{22}$	$U_{33}$	$U_{23}$	$U_{13}$	$U_{12}$
Pb	0.34125(3)	0.00490(4)	0.33909(2)	0.0125(1)	0.0089(2)	0.0134(2)	0.0152(2)	0.0012(1)	-0.0003(1)	0.0010(1)
Te	0.5000	0.5000	0.5000	0.0063(2)	0.0052(3)	0.0069(3)	0.0069(3)	0.0007(2)	0.0008(2)	-0.0002(2)
O1	0.5726(6)	0.7973(7)	0.4417(5)	0.013(1)	0.010(2)	0.008(2)	0.021(3)	0.010(2)	-0.002(2)	-0.002(2)
O2	0.4653(6)	0.3854(8)	0.3373(5)	0.014(1)	0.016(2)	0.020(3)	0.006(3)	-0.003(2)	0.000(2)	-0.007(2)
O3	0.2500	0.6256(10)	0.5000	0.010(1)	0.002(3)	0.010(3)	0.017(4)	0.000	0.002(3)	0.000

**TABLE 4.** Selected bond distances ( $\text{\AA}$ ) and angles ( $^\circ$ ) for ottoite

Pb-O2	2.367(4)	Te-O1 ( $\times 2$ )	1.899(4)
Pb-O1	2.368(4)	Te-O2 ( $\times 2$ )	1.902(5)
Pb-O2	2.533(5)	Te-O3 ( $\times 2$ )	2.016(2)
Pb-O1	2.595(4)	<Te-O>	1.939
Pb-O1	2.708(5)		
Pb-O3	2.881(4)	O1-Te-O2 ( $\times 2$ )	88.3(2)
Pb-O2	3.036(5)	O1-Te-O2 ( $\times 2$ )	91.7(2)
Pb-O1	3.560(5)	O1-Te-O3 ( $\times 2$ )	87.6(2)
Pb-O2	3.605(5)	O1-Te-O3 ( $\times 2$ )	92.4(2)
Pb-O2	3.661(5)	O2-Te-O3 ( $\times 2$ )	89.2(2)
Pb-O3	3.817(12)	O2-Te-O3 ( $\times 2$ )	90.8(2)
<Pb-O>	3.012	<O-Te-O>	90.0

**TABLE 5.** Bond valence analysis for ottoite. Values are expressed in valence units.

	O1	O2	O3	Sum
Pb	0.438 0.275	0.438 0.312	0.154 $\times 2 \downarrow$	2.075
	0.219 0.038	0.112 0.035	0.023 $\times 2 \downarrow$	
		0.031		
Te	1.050 $\times 2 \rightarrow$	1.041 $\times 2 \rightarrow$	0.765 $\times 2 \downarrow \rightarrow$	5.713
Sum	2.020	1.971	1.883	

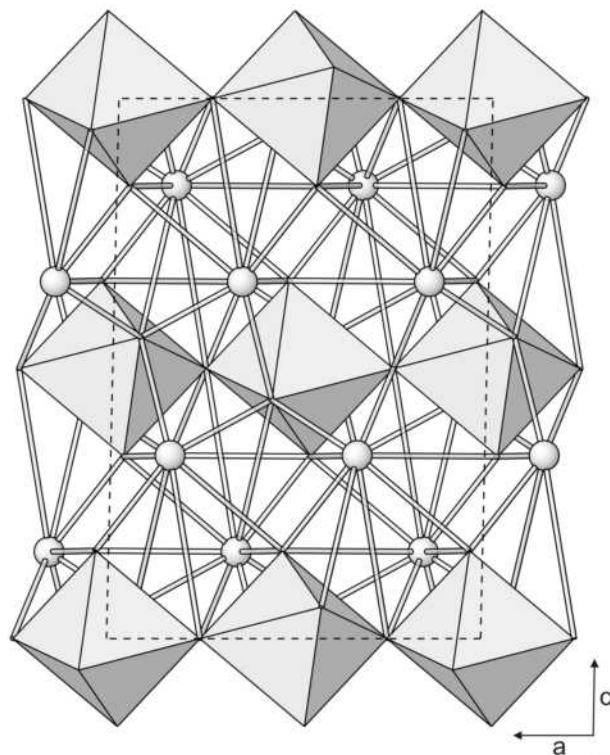
Notes: Multiplicity is indicated by  $\times \rightarrow \downarrow$ ;  $\text{Pb}^{2+}$ -O bond strengths from Krivovichev and Brown (2001);  $\text{Te}^{6+}$ -O bond strengths from Brown and Altermatt (1985).

As noted above, the structure of synthetic  $\text{Pb}_2\text{TeO}_5$  was solved from powder data by Wedel et al. (1998). There is little doubt that the structures of ottoite and synthetic  $\text{Pb}_2\text{TeO}_5$  are the same and that the cell and space group reported by Wedel et al. (1998) are in error. Their structure solution provides the same structural topology as ours, but significantly different bond distances and angles. The differences can be attributed both to the lower reliability of structure refinement from powder data and the wrong choice of cell and space group by Wedel et al. (1998).

A corner-sharing chain of  $\text{Te}^{6+}\text{O}_6$  octahedra is found in only one other mineral, housleyite (Kampf et al. 2010b); however, in housleyite the chain is made up of two distinct octahedra and the shared octahedral corners alternate between *cis* and *trans* configuration. Also, the chains in housleyite are linked into sheets by sharing edges and corners with  $\text{CuO}_6$  octahedra.

### COMPARISON WITH GIRDITE

The powder X-ray diffraction pattern of ottoite is quite similar to that of girdite, one of four new tellurium oxysalt minerals described from the Grand Central mine, Tombstone, Arizona, by Williams (1979). The girdite pattern has a few small extra peaks to that of ottoite and the matching peaks are generally shifted to slightly higher angles. The formula  $\text{H}_2\text{Pb}_3(\text{Te}^{4+}\text{O}_3)\text{Te}^{6+}\text{O}_6$  was provided based upon wet chemical analyses and water determination. Girdite was described as occurring in dense, chalky spherules with a "hint" of a crystalline druse on the surface. The spherules were noted to closely resemble those of oboyerite, one of the other new minerals described in the same paper. One "exceptional" specimen of girdite provided bow-tie

**FIGURE 6.** Structure of ottoite viewed along **b** showing the corner-sharing chains of  $\text{TeO}_6$  octahedra parallel to **a**. Pb atoms are shown as spheres.

aggregates of slender tapered prisms. From rotation and Weissenberg photographs on a small crystal fragment, Williams reported a monoclinic unit cell with  $a = 6.241$ ,  $b = 5.686$ ,  $c = 8.719$   $\text{\AA}$ , and  $\beta = 91^\circ 41'$ . Optical determinations in S-Se melts, also on crystal fragments, yielded the indices of refraction:  $\alpha = 2.44$ ,  $\beta = 2.47$ , and  $\gamma = 2.48$ . The density measured by Berman balance, presumably on the spherules, was  $5.5(2)$   $\text{g/cm}^3$  compared to a calculated density ( $Z = 1$ ) of  $5.49$   $\text{g/cm}^3$ .

To further investigate the relationship between ottoite and girdite, we obtained a sample of girdite from Richard Thomssen, which had been provided to him by S.A. Williams, and a sample of type girdite from The Natural History Museum, London (BM1980,539). Both samples fit the description of girdite as dense spherules coated with a thin crystalline druse. No distinct crystals or bow-tie aggregates are present on either sample.

Powder X-ray diffraction (PXRD) on the spherules provided a pattern more consistent with oboyerite than either girdite or ottoite. PXRD on a carefully separated sample of the crystalline crust yielded a pattern consistent with ottoite. Examination of the interior of the spherules by SEM-EDS indicated the likelihood that two phases are present. Electron microprobe analyses provided widely varying Pb:Te ratios from 1.12:1 to 1.67:1 with the average of the analyses: PbO 61.96 wt% and  $\text{TeO}_3$  32.54

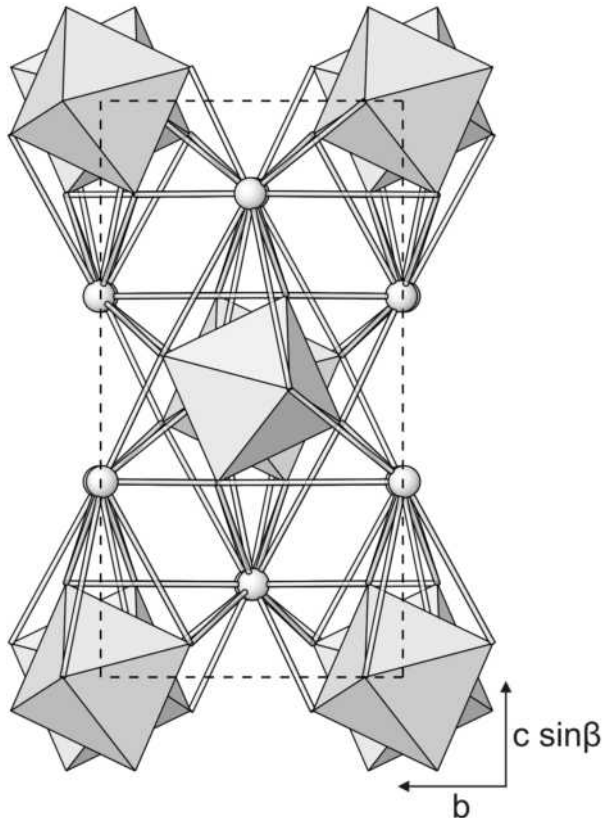


FIGURE 7. Structure of ottoite viewed along *a*, looking down the corner-sharing chains of  $\text{TeO}_6$  octahedra. Pb atoms are shown as spheres.

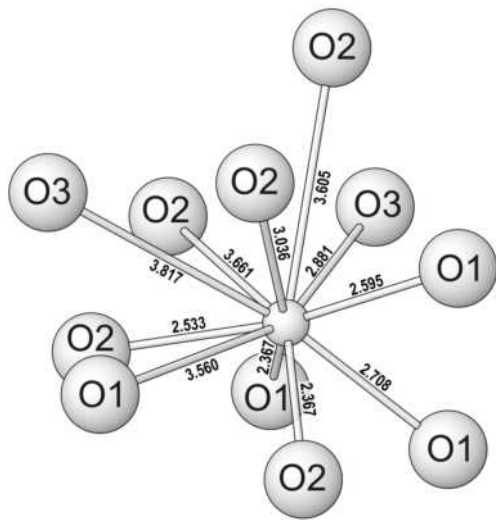


FIGURE 8. Coordination of the Pb atom in ottoite. The lopsided distribution of bond lengths is attributable to the localization of the lone-pair electrons. Bond lengths are given in angstroms.

wt%, total 96.50 wt%, very similar to the analyses reported by Williams (1979) and with Pb:Te close to 1.5:1. By comparison, Pb:Te for ottoite is ideally 2:1 and for oboyerite 1.2:1.

Taken at face value, the only data reported by Williams (1979) for girdite that are similar to those for ottoite are the PXRD data,

although the *b* cell length and  $\beta$  angle also are similar. It seems plausible that Williams based his description of girdite on data obtained from at least two and possibly three different phases, one of which may correspond to ottoite. His chemical analyses were conducted on the spherules, which may have been oboyerite, and which, in turn, may actually be a mixture itself. His PXRD may have been conducted on the crystals, rather than the spherules, and the crystals may correspond to ottoite; however, two lines of evidence argue against it: (1) there seems to be no obvious way to obtain his *a* and *c* cell parameters from a transformation of the ottoite cell, and (2) the average of the indices of refraction reported by Williams for the girdite crystals, 2.463, provides a very poor Gladstone-Dale compatibility of  $-0.154$  based on the formula, cell, and calculated density of ottoite.

#### ACKNOWLEDGMENTS

Pier F. Zanazzi, an anonymous reviewer, Technical Editor Ronald C. Peterson, and Associate Editor G. Diego Gatta are thanked for helpful comments on the manuscript and especially for suggestions regarding the crystal-structure refinement. Michael Rumsey is thanked for making available fragments from the type specimen of girdite in The Natural History Museum, London. Richard Thomssen is thanked for the loan of another specimen of girdite. The microprobe analyses were supported by a grant to the California Institute of Technology from the Northern California Mineralogical Association. The remainder of this study was funded by the John Jago Trelawney Endowment to the Mineral Sciences Department of the Natural History Museum of Los Angeles County.

#### REFERENCES CITED

- Altomare, A., Cascarano, G., Giacovazzo, C., Guagliardi, A., Burla, M.C., Polidori, G., and Camalli, M. (1994) SIR92—a program for automatic solution of crystal structures by direct methods. *Journal of Applied Crystallography*, 27, 435.
- Brown, I.D. and Altermatt, D. (1985) Bond-valence parameters from asystematic analysis of the inorganic crystal structure database. *Acta Crystallographica*, B41, 244–247.
- Cooper, M. and Hawthorne, F.C. (1994) The crystal structure of wherryite,  $\text{Pb}_7\text{Cu}_2(\text{SO}_4)_4(\text{SiO}_4)_2(\text{OH})_2$ , a mixed sulfate-silicate with  $[\text{M}(\text{TO}_4)_2\Phi]$  chains. *Canadian Mineralogist*, 32, 373–380.
- Crowley, J.A. (1977) Minerals of the Blue Bell mine, San Bernardino County, California. *Mineralogical Record*, 8, 494–496 and 518.
- Dowty, E. (2008) SHAPE, version 7.2. Shape Software, Kingsport, Tennessee, U.S.A.
- Grose, L. (1959) Structure and petrology of the northeast part of the Soda Mountains, San Bernardino County, California. *Geological Society of America Bulletin*, 70, 1509–1547.
- Grundler, P., Brugger, J., Meisser, N., Ansermet, S., Borg, S., Etschmann, B., Testemale, D., and Bolin, T. (2008) Xocolatlite,  $\text{Ca}_2\text{Mn}_2^+\text{Te}_2\text{O}_{12}\cdot\text{H}_2\text{O}$ , a new tellurate related to kuranakhite: Description and measurement of Te oxidation state by XANES spectroscopy. *American Mineralogist*, 93, 1911–1920.
- Holland, T.J.B. and Redfern, S.A.T. (1997) Unit cell refinement from powder diffraction data; the use of regression diagnostics. *Mineralogical Magazine*, 61, 65–77.
- Housley, R.M. (1997) Recent discoveries of talocite, kuksite, and other rare minerals from the Blue Bell Mine, San Bernardino County, California. *San Bernardino County Museum Association Quarterly*, 44, 9–12.
- Kampf, A.R., Rossman, G.R., and Housley, R.M. (2009) Plumbophyllite, a new species from the Blue Bell claims near Baker, San Bernardino County, California. *American Mineralogist*, 94, 1198–1204.
- Kampf, A.R., Housley, R.M., and Marty, J. (2010a) Lead-tellurium oxysalts from Otto Mountain near Baker, California: III. Thorneite,  $\text{Pb}_6(\text{Te}_2\text{O}_{10})(\text{CO}_3)\text{Cl}_2(\text{H}_2\text{O})$ , the first mineral with edge-sharing tellurate dimers. *American Mineralogist*, 95, in press.
- Kampf, A.R., Marty, J., and Thorne, B. (2010b) Lead-tellurium oxysalts from Otto Mountain near Baker, California: II. Housleyite,  $\text{Pb}_6\text{CuTe}_3\text{O}_{18}(\text{OH})_2$ , a new mineral with Cu-Te octahedral sheets. *American Mineralogist*, 95, 1337–1342.
- Kampf, A.R., Mills, S.J., Housley, R.M., Marty, J., and Thorne, B. (2010c) Lead-tellurium oxysalts from Otto Mountain near Baker, California: IV. Markcooperite,  $\text{Pb}_2(\text{UO}_2)\text{TeO}_6$ , the first natural uranyl tellurate. *American Mineralogist*, 95, in press.
- (2010d) Lead-tellurium oxysalts from Otto Mountain near Baker, California: V. Timroseite,  $\text{Pb}_2\text{Cu}_2^+(\text{Te}^{6+}\text{O}_6)_2(\text{OH})_2$ , and paratimroseite,  $\text{Pb}_2\text{Cu}_2^+(\text{Te}^{6+}\text{O}_6)_2(\text{H}_2\text{O})_2$ , new minerals with edge-sharing Cu-Te octahedral chains. *American Mineralogist*, 95, in press.
- (2010e) Lead-tellurium oxysalts from Otto Mountain near Baker, Cali-

- fornia: VI. Telluroperite,  $\text{Pb}_7\text{Te}^{4+}\text{O}_4\text{Cl}_2$ , the Te analog of perite and nadorite. *American Mineralogist*, 95, in press.
- Kharisun, Taylor, M.R., Bevan, D.J.M., Rae, A.D., and Pring, A. (1997) The crystal structure of mawbyite,  $\text{PbFe}_2(\text{AsO}_4)_2(\text{OH})_2$ . *Mineralogical Magazine*, 61, 685–691.
- Kraus, W. and Nolze, G. (1996) POWDER CELL—a program for the representation and manipulation of crystal structures and calculation of the resulting X-ray powder patterns. *Journal of Applied Crystallography*, 29, 301–303.
- Krivovichev, S.V. and Brown, I.D. (2001) Are the compressive effects of encapsulation an artifact of the bond valence parameters? *Zeitschrift für Kristallographie*, 216, 245–247.
- Mandarino, J.A. (1981) The Gladstone–Dale relationship. IV. The compatibility concept and its application. *Canadian Mineralogist*, 19, 441–450.
- Maynard, M.F., Valenti, A., Jenkins, J., Jenkins, F., Hall, D., Hall, J., White, B., White, S., Mansfield, M., and Mansfield, E. (1984) The Blue Bell Claims, San Bernardino County, California, p. 61. San Bernardino County Museum, Redlands, California.
- Mills, S.J., Groat, L.A., and Kolitsch, U. (2008) Te, Sb and W mineralization at the Black Pine mine, Montana. Poster, 18th Annual V.M. Goldschmidt Conference, Vancouver, Canada, July 13–18, 2008; abstract in *Geochimica et Cosmochimica Acta* 72, Special Supplement 12S, A632.
- Mills, S.J., Kampf, A.R., Raudsepp, M., and Christy, A.G. (2009a) The crystal structure of Ga-rich plumbogummite from Tsumeb, Namibia. *Mineralogical Magazine*, 73, 837–845.
- Mills, S.J., Kolitsch, U., Miyawaki, R., Groat, L.A., and Poirier, G. (2009b) Joëlbruggerite,  $\text{Pb}_2\text{Zn}_3(\text{Sb}^{5+}, \text{Te}^{6+})\text{As}_2\text{O}_{13}(\text{OH}, \text{O})$ , the  $\text{Sb}^{5+}$  analog of dugganite, from the Black Pine mine, Montana. *American Mineralogist*, 94, 1012–1017.
- Mills, S.J., Kampf, A.R., Kolitsch, U., Housley, R.M., and Raudsepp, M. (2010) The crystal chemistry and crystal structure of kuksite,  $\text{Pb}_2\text{Zn}_3\text{Te}^{6+}\text{P}_2\text{O}_{14}$ , and a note on the crystal structure of yafsoanite,  $(\text{Ca}, \text{Pb})_3\text{Zn}(\text{TeO}_6)_2$ . *American Mineralogist*, 95, 933–938.
- Moore, P.B. (1988) The joesmithite enigma: Note on the  $6s^2 \text{Pb}^{2+}$  lone pair. *American Mineralogist*, 73, 843–844.
- Sheldrick, G.M. (2008) A short history of SHELX. *Acta Crystallographica*, A64, 112–122.
- Speck, A.L. (2001) PLATON, a multipurpose crystallographic tool. Utrecht University, Utrecht, The Netherlands, <http://www.cryst.chem.uu.nl/platon>.
- Walker, J.D. and Wardlaw, B.R. (1989) Implications of Paleozoic and Mesozoic rocks in the Soda Mountains, northeastern Mojave Desert, California, for late Paleozoic and Mesozoic Cordilleran orogenesis. *Geological Society of America Bulletin*, 101, 1574–1583.
- Wedel, B., Wulff, L., and Müller-Buschbaum, H. (1998) Isolated  $[\text{TeO}_5]$  chains of octahedra in the lead tellurate  $\text{Pb}_2\text{TeO}_5$ . *Zeitschrift für Naturforschung*, 53b, 287–290.
- Williams, S. (1979) Girdite, oboyerite, fairbankite, and winstanleyite, four new tellurium minerals from Tombstone, Arizona. *Mineralogical Magazine*, 43, 453–457.

MANUSCRIPT RECEIVED JANUARY 27, 2010

MANUSCRIPT ACCEPTED APRIL 12, 2010

MANUSCRIPT HANDLED BY G. DIEGO GATTA